

Supporting Information

General

^1H NMR spectra were recorded with a JEOL JNMGSX-400 spectrometer. XRD patterns were measured with Rigaku RINT InPlane/ultraX18SAXS-IR using CuK_α radiation. The voltage was set to 40 kV, and the current was set to 200 mA. IR spectra were measured on a Horiba FT-710 spectrometer.

Chemical shifts of 1-PTHF precipitate

$^1\text{H-NMR}$ (DMSO- d_6) δ 1.48-1.51 (m, 14H), 2.91 (t, 1H, $J = 8.43$ Hz), 2.99-3.06 (m, 4H), 3.12 (dd, 1H, $J = 8.06$, 3.3Hz), 3.18-3.79 (m, 97H), 4.03-4.08 (m, 1H), 4.59 (d, 1H, $J = 7.7$ Hz), 4.97 (m, 4H), 5.40 (d, 1H, $J = 3.3$ Hz).

Chemical shifts and ^1H NMR spectrum of 2-PTHF precipitate

$^1\text{H-NMR}$ (DMSO- d_6) δ 1.48-1.51 (m, 6H), 3.00 (dd, 6H, $J = 9.9$, 3.3 Hz), 3.23 (s, 18H), 3.32-3.53 (m, 60H), 3.69-3.77 (m, 12H), 4.96 (d, 6H, $J = 3.3$ Hz).

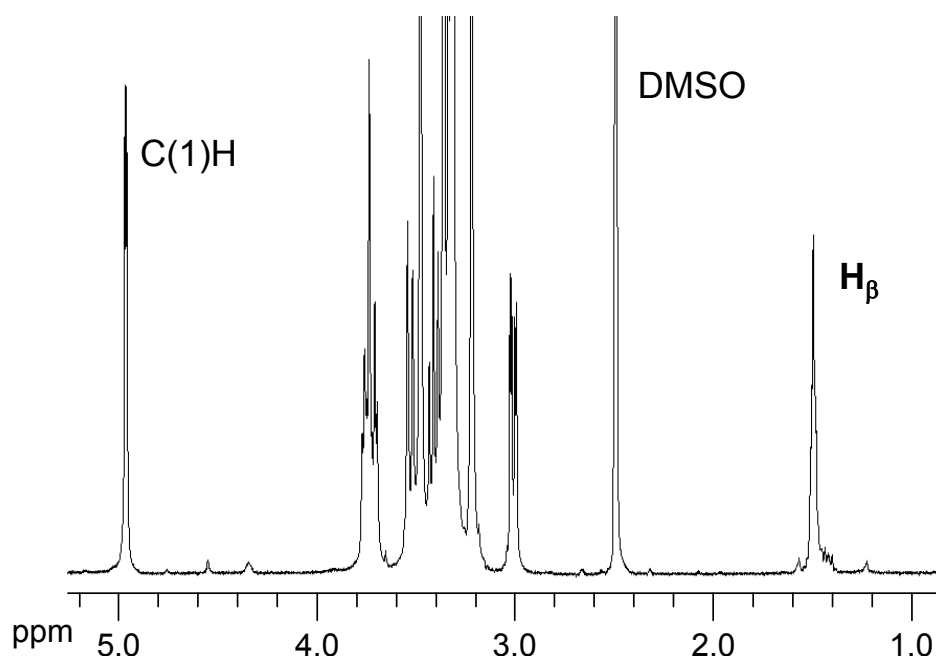


Figure S1. ^1H NMR spectrum of the **2**-PTHF precipitate in DMSO- d_6 at 25 °C.

XRD patterns, Chemical shifts, and ^1H NMR spectrum of 1-PCL precipitate

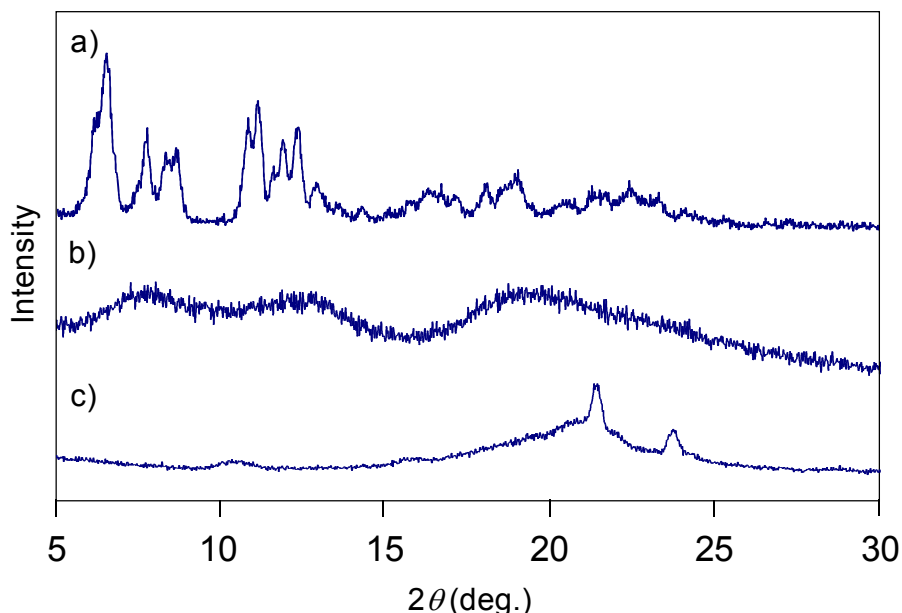


Figure S2. XRD patterns of a) 1-PCL precipitate, b) 1, and c) PCL.

$^1\text{H-NMR}$ (DMSO- d_6) δ 1.22-1.32 (m, 9H), 1.48-1.58 (m, 18H), 2.23-2.28 (m 9H), 2.91 (t, J = 8.43 Hz, 1H), 2.99-3.06 (m, 4H), 3.12 (dd, 1H, J = 8.06, 3.3Hz), 3.18-3.79 (m, 83H) ,3.97 (t, 9H, J = 6.6 Hz), 4.03-4.08 (m, 1H), 4.59 (d, 1H, J = 7.7 Hz), 4.97 (m, 4H), 5.40 (d, 1H, J = 3.3 Hz).

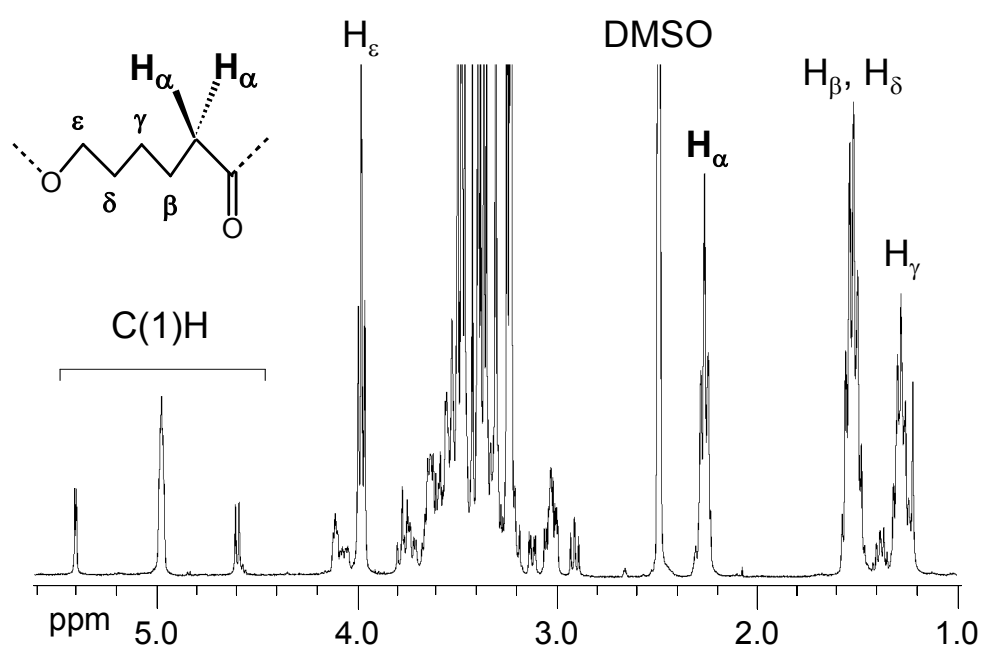


Figure S3. ^1H NMR spectrum of the 1-PCL precipitate in DMSO- d_6 at 25 °C.

XRD patterns, Chemical shifts and ^1H NMR spectrum of 2-PCL precipitate

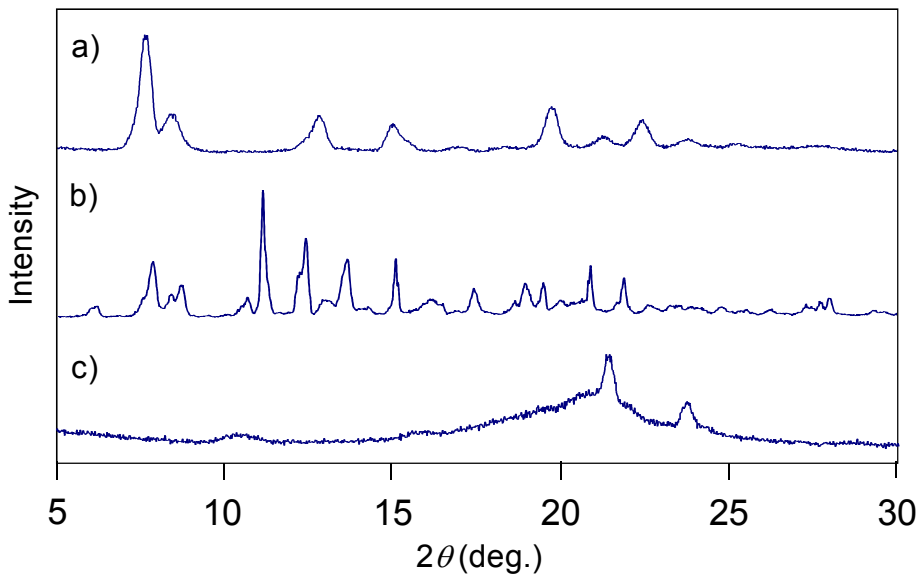


Figure S4. XRD patterns of a) 2-PCL precipitate, b) **2**, and c) PCL.

$^1\text{H-NMR}$ ($\text{DMSO}-d_6$) δ 1.22-1.32 (m, 2H), 1.48-1.58 (m, 4H), 2.32-2.3 (m, 2H), 3.00 (dd, 6H, $J = 9.9, 3.3$ Hz), 3.22 (s, 18H), 3.31-3.53 (m, 54H), 3.69-3.77 (m, 12H), 3.97 (t, 2H, $J = 6.6$ Hz), 4.96 (d, 6H, $J = 3.3$ Hz).

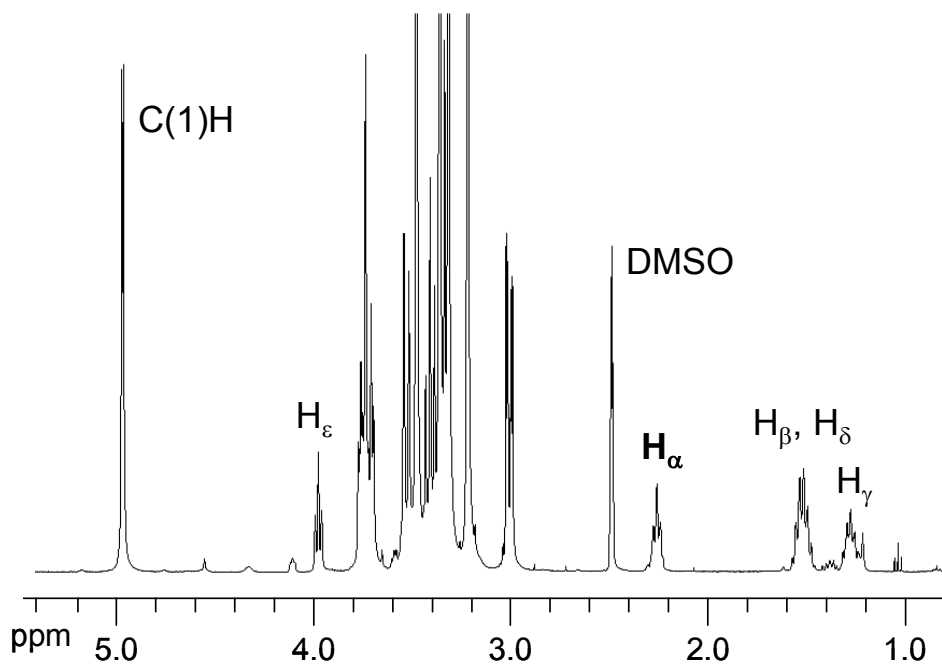


Figure S5. ^1H NMR spectrum of the **2**-PCL in $\text{DMSO}-d_6$ at 25 °C.

Chemical shifts of 1-PAA precipitate

$^1\text{H-NMR}$ (DMSO- d_6) δ 1.16-1.66 (m, 10H), 2.20 (m, 5H), 2.91 (t, $J = 8.43$ Hz, 1H), 2.99-3.06 (m, 4H), 3.12 (dd, 1H, $J = 8.06$, 3.3Hz), 3.18-3.79 (m, 83H) , 4.03-4.08 (m, 1H), 4.59 (d, 1H, $J = 7.7$ Hz), 4.97 (m, 4H), 5.40 (d, 1H, $J = 3.3$ Hz), 12.25 (m, 10H).

XRD patterns, Chemical shifts, and ^1H NMR spectrum of 1-PPG precipitate

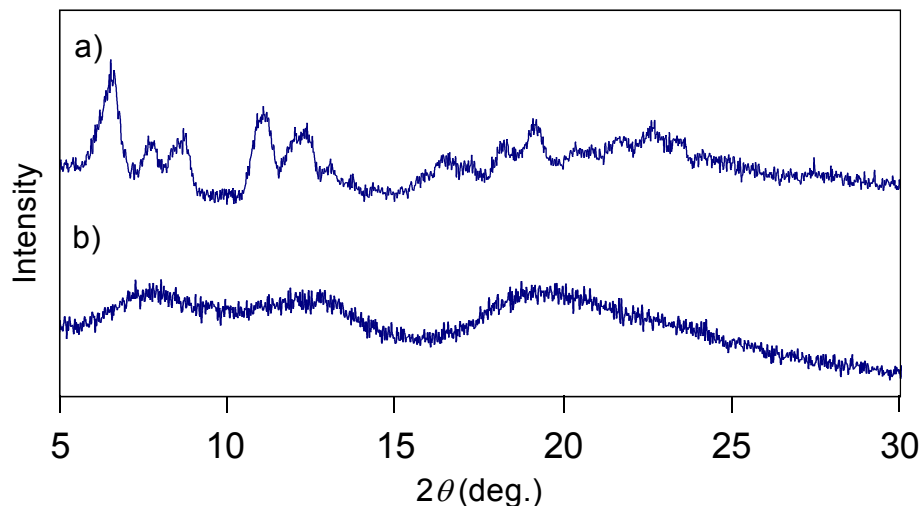


Figure S6. XRD patterns of a) 1-PPG precipitate and b) **1**.

$^1\text{H-NMR}$ (DMSO- d_6) δ 1.03 (d, 6H, $J = 6.2$ Hz), 2.91 (t, $J = 8.43$ Hz, 1H), 2.99-3.06 (m, 4H), 3.12 (dd, 1H, $J = 8.06$, 3.3Hz), 3.18-3.79 (m, 89H) , 4.03-4.08 (m, 1H), 4.59 (d, 1H, $J = 7.7$ Hz), 4.97 (m, 4H), 5.40 (d, 1H, $J = 3.3$ Hz).

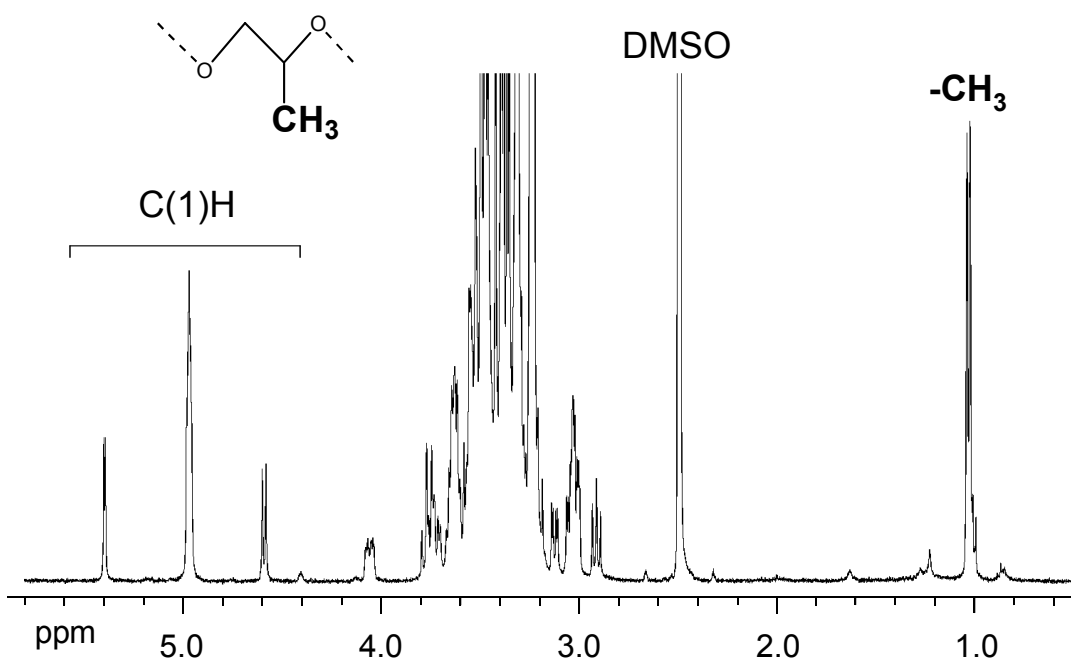


Figure S7. ^1H NMR spectrum of the 1-PPG precipitate in $\text{DMSO}-d_6$ at 25°C .

XRD patterns, Chemical shifts, and ^1H NMR spectrum of 2-PPG precipitate

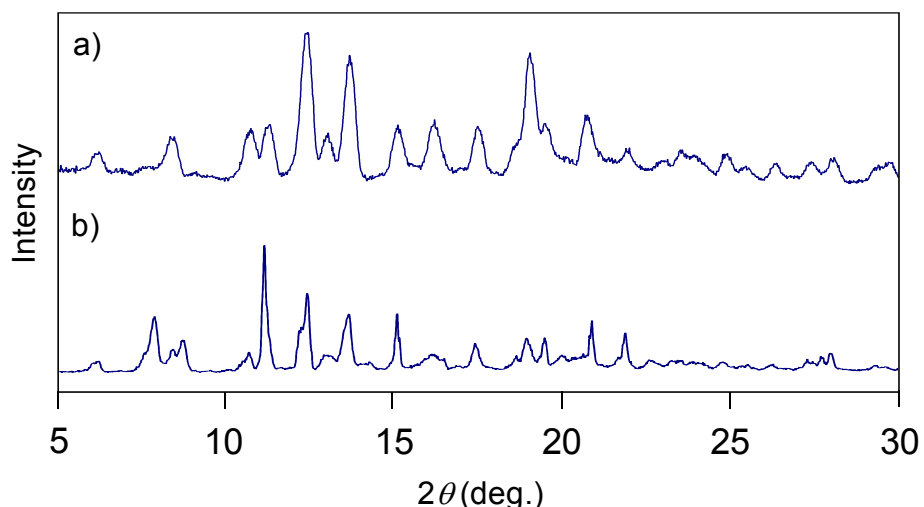


Figure S8. XRD patterns of a) 2-PPG precipitate and b) 2.

$^1\text{H-NMR}$ ($\text{DMSO}-d_6$) δ 1.02 (d, 17H, $J = 7.0$ Hz), 3.00 (dd, 6H, $J = 9.6, 3.1$ Hz), 3.21 (s, 18H), 3.30-3.54 (m, 71H), 3.68-3.78 (m 12H), 4.96 (d, 6H, $J = 3.3$ Hz).

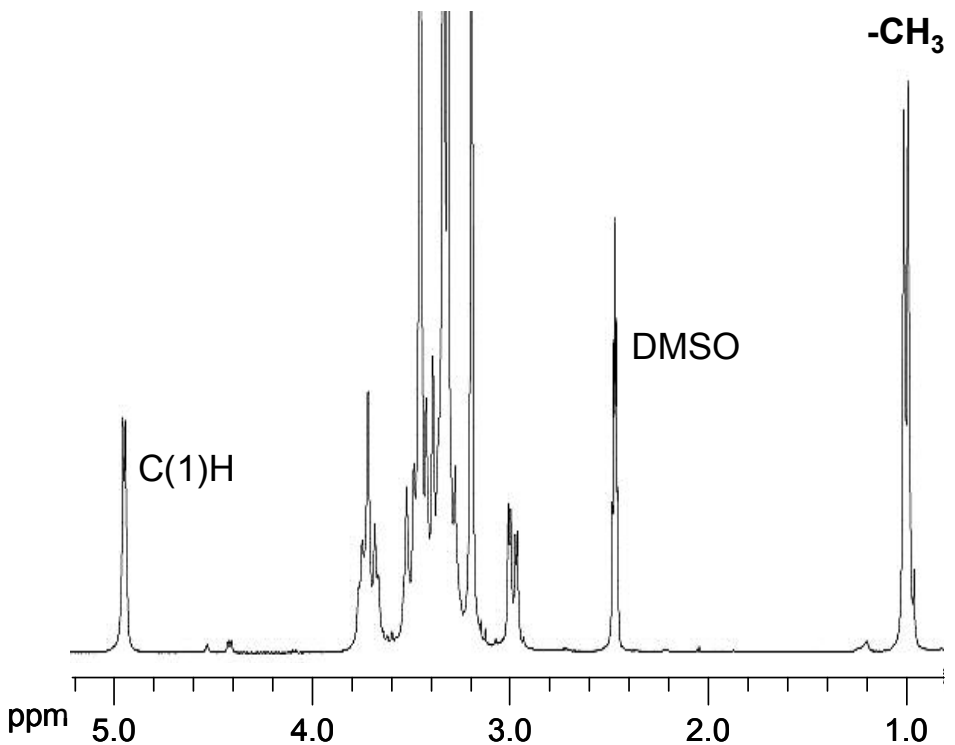


Figure S9. ^1H NMR spectrum of the **2**-PPG precipitate in $\text{DMSO}-d_6$ at 25 °C.